



HAL
open science

In-cell investigation of the conformational landscape of the GTPase UreG by SDSL-EPR

Annalisa Pierro, Ketty C Tamburrini, Hugo Leguenno, Guillaume Gerbaud, Emilien Etienne, Bruno Guigliarelli, Valérie Belle, Barbara Zambelli, Elisabetta Mileo

► To cite this version:

Annalisa Pierro, Ketty C Tamburrini, Hugo Leguenno, Guillaume Gerbaud, Emilien Etienne, et al.. In-cell investigation of the conformational landscape of the GTPase UreG by SDSL-EPR. *iScience*, 2023, <10.1016/j.isci.2023.107855>. <hal-04233485>

HAL Id: hal-04233485

<https://hal.science/hal-04233485v1>

Submitted on 9 Oct 2023

HAL is a multi-disciplinary open access archive for the deposit and dissemination of scientific research documents, whether they are published or not. The documents may come from teaching and research institutions in France or abroad, or from public or private research centers.

L'archive ouverte pluridisciplinaire HAL, est destinée au dépôt et à la diffusion de documents scientifiques de niveau recherche, publiés ou non, émanant des établissements d'enseignement et de recherche français ou étrangers, des laboratoires publics ou privés.



HAL Authorization

In-cell investigation of the conformational landscape of the GTPase UreG by SDSL-EPR.

Annalisa Pierro,^{1,2,7} Ketty Concetta Tamburrini,^{3,4,7} Hugo Leguenno,⁵ Guillaume Gerbaud,¹ Emilien Etienne,¹ Bruno Guigliarelli,¹ Valérie Belle,¹ Barbara Zambelli^{6,*} and Elisabetta Mileo^{1,8*}

¹Aix Marseille Univ, CNRS, BIP, IMM, 13009, Marseille, France.

²Department of Chemistry, University of Konstanz, Universitätsstraße 10, 78457 Konstanz, Germany.

³Aix Marseille Univ, CNRS, AFMB, 13009, Marseille, France.

⁴INRAE, Aix Marseille Univ, BBF, 13009, Marseille, France.

⁵Aix Marseille Univ, CNRS, BIP, IMM, 13009, Marseille, France.

⁶Laboratory of Bioinorganic Chemistry, Department of Pharmacy and Biotechnology, University of Bologna, 40127, Bologna, Italy.

⁷These authors contributed equally.

⁸Lead contact.

*Correspondence: barbara.zambelli@unibo.it (B.Z.) and emileo@imm.cnrs.fr (E.M.)

Summary: UreG is a cytosolic GTPase involved in the maturation network of urease, a Ni-containing bacterial enzyme. Previous investigations *in vitro* showed that UreG features a flexible tertiary organization, making this protein the first enzyme discovered to be intrinsically disordered. To determine whether this heterogeneous behavior is maintained in the protein natural environment, UreG structural dynamics was investigated directly in intact bacteria by *in-cell* EPR. This approach, based on site-directed spin labeling coupled to electron paramagnetic resonance (SDSL-EPR) spectroscopy, enables the study of proteins in their native environment.

The results show that UreG maintains heterogeneous structural landscape *in-cell*, existing in a conformational ensemble of two major conformers, showing either random coil-like or compact properties. These data support the physiological relevance of the intrinsically disordered nature of UreG and indicates a role of protein flexibility for this specific enzyme, possibly related to the regulation of promiscuous protein interactions for metal ion delivery.

Introduction

Molecular chaperones are essential players for cellular life because they regulate protein folding, interaction, activity and degradation, all functions that guarantee protein homeostasis. From a structural point of view, their activity implies a sequence of transient, reversible, and promiscuous protein–protein interactions, which are often promoted by fold flexibility. The chaperone UreG assists the activation of urease, a nickel-dependent enzyme produced by bacteria, archaea, fungi and plants, with important applications for health and agriculture.¹ UreG couples the role as molecular chaperone with an enzymatic role as a GTPase. In ureolytic bacteria, it generally collaborates with three other urease-chaperones (UreF, UreD and UreE) and couples the energy derived from the GTP hydrolysis to Ni(II)

transfer from the metallochaperone UreE towards the platform constituted by UreF and UreD, which eventually delivers Ni(II) to the active site of urease containing a lysine carbamylated in this process.²

Crystallographic structures of UreG, in the UreD₂-UreF₂-UreG₂*GDP complex (PBD: 4HI0) from *Helicobacter pylori*³ and in the UreG₂*GMPPNP-Ni(II) (guanylyl imidodiphosphate, a non-hydrolyzable GTP analogue) complex (PBD: 5XKT) from *Klebsiella pneumoniae*,⁴ show UreG in a dimeric well-folded structure. Differently, in vitro studies, including circular dichroism, intrinsic fluorescence, differential scanning calorimetry, NMR and native mass spectrometry, revealed that in solution the protein behaves as an ensemble of heterogeneous conformations, featuring different degrees of secondary and tertiary organization.^{5,6,7,8,9} The structural flexibility observed for UreG made this protein the first enzyme discovered to be intrinsically disordered (ID) under native conditions.^{10,11} Previously, we applied Site-Directed Spin Labeling coupled to Electron Paramagnetic Resonance spectroscopy (SDSL-EPR) to study local dynamics of UreG (from *Sporosarcina pasteurii*, *SpUreG*, and *Helicobacter pylori*, *HpUreG*) in diluted solution.^{12,13} SDSL-EPR investigations are based on the insertion of paramagnetic moieties (e.g. nitroxides, metal-based tags and trityls) in a specific position of a biomolecule.¹⁴⁻¹⁸ For proteins, cysteine residues are usually employed for label grafting, but tyrosine residues can also be targeted.¹⁹⁻²¹ When nitroxide labels are used, the labeled protein can be studied by different EPR approaches, such as continuous-wave EPR (CW-EPR) and Double Electron-Electron Resonance (DEER).^{22,23} The major asset of CW-EPR experiments is that the EPR spectral shape of nitroxides is highly related to their mobility. This provides information about protein local dynamics, that can be studied in solution and at room temperature. DEER experiments allow to measure distance distributions between two spin labels in the range of 2-8 nm, and the experiments are carried out in frozen solution because of the fast-relaxing properties of spin labels. The SDSL-EPR study of *SpUreG* and *HpUreG* revealed that a compact and an extended conformers are in equilibrium in solution, their presence being modulated by nickel ions or GTP-like substrates^{12,13} and that UreG exists in a concentration-dependent monomer/dimer equilibrium, which does not affect its intrinsically disordered state in solution.¹² The well-folded structure found in the crystal state contrasts with the natively flexible state observed in solution, which suggests that the protein acquires a rigid structure only upon binding of its partners. To demonstrate whether this latter behavior is maintained in the natural setting, the conformational state of the protein inside the bacterial cells must be investigated.

The present work unravels the fold and dynamics of *SpUreG* directly in the interior of bacterial cells, by *in-cell* SDSL-EPR. This technique is a recent approach enabling the study of protein structural dynamics directly inside cells.^{14,24,25} The use of nitroxide-based spin labels allowed running EPR analysis at room temperature, at conditions compatible with the life of the cells under investigation.²⁶ To study proteins in their native environment, different alternatives are currently available: the spin-labeled protein can be delivered or synthesized directly inside cells²⁷⁻³² and the impact of the cellular environment can be studied by EPR spectroscopy in cells maintained in suspension in a hydrogel and at room-temperature.³³ The majority of protocols available to deliver spin-labeled proteins inside cells employs a finely tuned electroporation method.^{28,34-36} Here, *SpUreG* delivery was achieved by modifying a protocol based on the thermal treatment of bacterial cells recently published,³¹ which enabled to strongly improve *SpUreG* intracellular delivery. The results show that *SpUreG* maintains structural flexibility and heterogeneous landscape *in-cell*, existing in a conformational ensemble of two major conformers, showing either extended or compact properties, both *in-cell* and in solution. Notably, the cellular environment mostly affects the compact

conformation, decreasing its mobility and improving its rigidity, while the random coil-like conformation remains almost unaffected. The obtained data support the physiological relevance of the ID nature of the GTPase SpUreG.

Results and Discussion

1. SpUreG structural dynamics investigated in vitro by EPR spectroscopy.

To study SpUreG by SDSL-EPR, we prepared several Cys-variants which were conjugated with a paramagnetic spin label selective for thiol groups, the maleimido-proxyl nitroxide (**1**) (here named “M-Proxyl”, Figure 1A). SpUreG (Figure 1B) presents one native cysteine (Cys68) available for labeling, in the Cys-Pro-His metal binding site¹² making the wild-type protein useful for grafting spin label **1** (C68^{proxyl}) and monitoring this region of the protein. Other two variants introduced a Cys for labeling in the proximity of the N-terminus P-Loop (Gly-Ser-Gly-Lys-Thr) GTP binding motif (G9C^{proxyl}) or in the C-terminus of the protein (D158C^{proxyl}), which is involved in the interaction with the chaperone partner UreE.³ In the latter two variants, Cys68 was mutated in alanine (Cys68Ala) to selectively label only a single position of the protein.^{5,37} A double cysteine variant (G9C^{proxyl}/D158C^{proxyl}) served to probe distance distributions between the two spin centers by DEER experiments. The labeling efficiency was over 90% for all variants as confirmed by comparing the double integration of the EPR spectra with the protein concentration and confirmed by mass spectrometry (Figure S1).

EPR spectra of SpUreG variants G9C^{proxyl}, C68^{proxyl} and D158C^{proxyl} (Figure 2 A, B, C) showed multicomponent spectra suggesting that at least two different spectral components coexist. The simulation of experimental data^{38,39} (Figure 2, panels M, N, O), indicated that all variants present a *sharp* component and a *broad* component of the spectrum: the *sharp* component is characterized by a rotation correlation time (τ_c) $\tau_c \leq 1$ ns, typical of unstructured regions.^{27,40} The *broad* component is characterized by a higher correlation time that differs between the three variants: in particular, the τ_c of the broad component is significantly lower for C68^{proxyl} (4.0 ns) than for the other two variants (6.5 ns for D158C^{proxyl}; 7.5 ns for G9C^{proxyl}).¹² While the *broad* and *sharp* components are equally represented for the C68^{proxyl}, both G9C^{proxyl} and D158C^{proxyl} show a prevalence of the broad component (Figure 2M, N, O). These results reflect the co-existence of multiple protein substates, initially revealed by the large line broadening of NMR spectra of UreG from multiple sources, the latter indicative of conformational equilibria in the intermediate exchange regime that, for NMR, is typically in the millisecond to microsecond timescale.^{5,7,9,10,41} This was subsequently confirmed by native mass spectrometry⁸ and by SDSL-EPR,^{12,13} which also found that several osmolytes perturb protein folding.¹² In this work, the effect of PEG and sucrose on the spectral shape of all the variants was demonstrated (Figure 2 and Figure S7).⁴²⁻⁴⁴

Concerning the two protein substates, one results more compact and mostly found in the proximity of the protein core and of the GTP-binding region, the other disordered and more abundant in the surrounding of the metal-binding domain.

2. SpUreG local dynamics in cellular context.

2.1 - Delivery of spin labeled UreG into E. coli cells. In-cell EPR experiments are conducted by prior labeling the protein of interest, produced by recombinant expression, and by delivering it inside cells.^{24,36} Recently, we investigated the structural dynamics of the bacterial protein NarJ in its native environment, E. coli cells. The delivery of labeled NarJ into bacteria was achieved by electroporation.³⁴ Here an alternative and recently reported delivery protocol,

based on thermal shock,^{31,32} was adapted for the delivery of *SpUreG* and compared to electroporation. In particular, Ca(II) ions, in combination with a short incubation at 42 °C, were used to trigger protein delivery (Figure S2). Ca(II) ions are necessary for protein internalization: in the absence of Ca(II) no internalization can be detected (Figure S3).

Ca(II) is a known precipitating agent, its concentration should be carefully evaluated. The set-up of this parameter was done using the super-folded (*sf*)GFP as a model system and the internalization of the protein was followed by fluorescence microscopy (Figure 3 and Figure S4). Addition of 50 mM CaCl₂ caused protein aggregation around the bacteria (Figure 3A); differently, in the presence of 10 mM CaCl₂, the protein was properly internalized and no aggregates are visible (Figure 3B). Coherently, the average fluorescence, measured for each bacterium, normalized to the background of the image (Figure S5) shows that bacteria acquire significantly more GFP when they are treated with 10mM CaCl₂ than with 50 mM, because the aggregates outside the cells decrease the signal to noise ratio. The non-specific interaction of the protein with the cell membrane was excluded by the absence of fluorescence for a sample not subjected to the thermal treatment in the presence of 10 mM CaCl₂ (Figure 3C, S4 and S6). Cell viability was not affected by the presence of 10 mM CaCl₂ (Figure S7). Therefore, 10mM of Ca(II) was chosen as optimal concentration to exogenously deliver *SpUreG* by thermal shock into cells.

EPR spectra obtained by delivering all the *SpUreG* variants into *E. coli* cells by electroporation (Figure 4A, B, C) and thermal shock (Figure 4D, E, F), applied to the same number of cells (4-7 x 10¹⁰ cells/mL), show that the former protocol is not efficient, and that the amount of *SpUreG* delivered into cells was insufficient to provide good EPR signal-to-noise ratio. Differently, thermal shock provided ~20-fold higher EPR signal-to-noise ratio and sensibly reduced the acquisition time window from 50 minutes to 1-15 minutes, according to the spectral shape obtained.

Reducing the acquisition time is important to preserve the viability of the bacteria under investigation and to limit the decrease of intracellular nitroxide signal over time, due to its cytosolic reduction to hydroxylamine, a silent EPR derivative.^{24,45} No significant changes of EPR spectral shapes of the *SpUreG* variants delivered by heat-shock or by electroporation were observed, indicating that the *in-cell* EPR data depend to the cellular environment and not to the delivery method. All these considerations prompted us to use the thermal shock protocol for the preparation of all *in-cell* samples. This comparative analysis points out the importance of individually optimizing the delivery methods for different exogenous protein into the cells.

2.2 - Local structural dynamics of *SpUreG* in the cellular context. The EPR spectra of all *SpUreG* variants delivered into the bacterial cells (Figure 2D, E, F) are characterized by a general broadening of line-shapes as compared to the *in vitro* samples (Figure 2A, B, C), indicating a decrease of nitroxide mobility. Quantitative simulations of the spectra (Figure 2M, N, O) indicated that the protein landscape maintains its heterogeneity in the bacterial cytoplasm and can be dissected into two different conformations, represented by a *sharp* and a *broad* component, as reported *in vitro*. A component-dependent response to the cellular environment was observed: the τ_c of the *broad* component increases of ca. 1.5 times, reaching values close to what expected for well-folded and rigid protein regions; differently, the sharp component maintains very low values of τ_c typical of disordered regions (Table S1). The relative amount between the *sharp* and *broad* components, slightly shifts toward the *broad* one in all the labeled positions, indicating an increased ratio of the most compact conformations.

Overall, position C68 is the one characterized by the higher fraction of fast-dynamics component, while the other two positions, while G9C and D158C are characterized by a lower fraction, with a trend that is similar to the one found in solution. This conformational response to the cellular environment is remarkably different from the one we previously observed for NarJ, another flexible chaperone with a similar molecular weight, whose structural dynamics was affected strongly and in a site-specific way by the cytosolic environment, with τ_c variations strictly related to the investigated region.

The conformational response of SpUreG to the cellular environment was further investigated, analyzing the behavior of structural dynamics in highly concentrated crowder solutions containing polymers, sugars and osmolytes often used to mimic, *in vitro*, cellular confinement, non-specific interactions and charge-charge repulsion that proteins experience in the cytoplasm.^{46,47} In particular, we tested *i*) two synthetic polymers, polyethylene glycol (PEG) and Ficoll that behave like semi-rigid spheres, thus mimicking globular macromolecules;^{48,49} *ii*) their corresponding monomers, sucrose and ethylene glycol, respectively;⁴⁷ and *iii*) Bovine Serum Albumin (BSA), which mimics non-specific protein-protein interactions.⁵⁰ These molecules only slightly affected the spectral features of SpUreG variants (Figure S8A) with the exception of PEG8000 and sucrose (Figure 2). Results of quantitative simulation of the spectra (Figure S8B) indicated that, as the cellular environment, the crowding agents mostly impacted on the dynamics of the *broad* component, with τ_c shifting towards higher values, while the *sharp* component was only slightly affected. In the case of “protecting agents”, such as PEG, Ficoll and sucrose, this result is not surprising because they have already been shown to stabilize protein folding by lowering the energy of the least hydrated conformer.^{51,52}

PEG8000 and sucrose induced spectral changes very similar to those observed *in-cell*, with the correlation time of the broad component increasing by 2 ns for C68^{proxyl} and D158C^{proxyl} and 1 ns for G9C^{proxyl}. Differently, Ficoll and EthG promoted an increase of the relative amount of the *broad* component in G9C^{proxyl}, and induced only a mild effect on the other two variants. BSA effected only the D158C^{proxyl} variant promoting a slight stabilization of the broad component.

Nitroxide reduction in the cytosol during time: In the cytosol, nitroxides are reduced to the corresponding EPR silent hydroxylamine under the action of enzymes and antioxidants, such as glutathione.^{24,45} Reduction rates of nitroxide-labels, obtained by following the intensity of the EPR signal inside cells upon time, are proportional to the accessibility of the site to which the nitroxide is grafted. The more the nitroxide is reduced, the more the site results to be accessible to the reductants. For example, in our previous study on NarJ chaperone, it undergoes to important structural changes *in-cell* that affect the reduction rate of the grafted nitroxide, in a site-dependent way, with the most buried sites being those showing the slower reduction.³⁴ For SpUreG, all variants are reduced at the same rate *in-cell* (Figure 5), indicating that the accessibility of the reducing agent is similar for all the labeled positions and clearly supporting a diffuse structural flexibility of SpUreG tertiary structure in the cytosol.

3. SpUreG conformational ensemble by DEER-EPR. Distances between different protein regions were obtained applying DEER-EPR on the doubly labeled SpUreG G9C^{proxyl}/D158C^{proxyl} *in vitro* and in *E. coli* cells. *In vitro*, the absence of oscillation in the time trace (Figure S9A, B) results in a large distance distribution (Figure S9C) which spans a broader range than those predicted by MMM calculation,⁵³ from the available HpUreG crystal structure (Figure S9C, *green area*). In the case of distance distributions characterized by a full-width at half-maximum (FWHM) larger than 20 Å this indicates high protein flexibility and in our case that

the two labels attached to the protein are not on rigid positions but move one respect to the other along the tertiary structure, supporting the existence of a conformational ensemble in solution.

Concerning *in-cell* experiments, the sample was prepared by delivering the doubly labeled variant inside *E. coli* cells via the heat-shock protocol described before. Approximately ~15 minutes after the thermal shock, the sample was shock-frozen in liquid nitrogen to perform DEER experiments at 60 K. *In-cell* DEER traces presented a good signal to noise ratio and modulation depth in the cellular environment (Figure 6A), but the reliability distance distributions was compromised by the short phase memory relaxation time (T_m), that was 0,3 μ s in cell versus 3 μ s, measured in solution (Figure S10A). Short T_m values in the cellular context have already been observed for other proteins.^{54,55} An evaluation of the form factor of the raw data and of the shape of distance distribution, as well as a comparison with the *in vitro* data (Figure 6B), indicated that the protein maintains a high flexibility of its tertiary structure in cell.

The fact that in this work, the CW-EPR study in cells reveals that UreG gains structure is not in contradiction with the DEER results, simply because they give information about different structural level of the protein under investigation. The high flexibility in the tertiary structure of UreG is also confirmed by the result of the nitroxide reduction inside cells.

4. Conclusions

Previous studies demonstrated that, in solution, the GTPase *SpUreG* populates at least two conformational states: a compact one and a random coil-like one, whose prevalence in solution could be modulated by denaturants or osmolytes.¹² Three singly-labeled variants of UreG, (C68^{proxyl}, G9C^{proxyl}, D158C^{proxyl}) were used to monitor different regions of the protein tertiary structure. The EPR spectra show that, in solution, different regions of the protein experience a similarly heterogeneous conformational landscape, with the more compact conformation being prevalent around the catalytic core (G9), while the metal-binding site (C68) of the protein shows a higher backbone flexibility, similarly to what previously observed for *HpUreG*.¹³

Is this conformational equilibrium conserved in the physiological environment? To answer this question, we investigated the local and global dynamics of *SpUreG* in the cytoplasm of *E. coli* cells. The properties of nitroxide labels to sample protein local dynamics by EPR spectroscopy at room temperature, the development of efficient intracellular delivery method for labeled proteins allowed us to observe that both compact and flexible conformations exist in the cellular environment, represented by the *broad* and a *sharp* components of the *in-cell* EPR spectra, similar to those found in solution. The compact conformer is most affected by the cellular environment, showing a significant reduction of the protein mobility in all the studied positions. This change in protein dynamics can be attributed either to the acquisition of additional structural elements or to the compaction of the existing structures by tertiary contacts. However, the protein does not acquire a fully-compact state *in-cell*: the equal accessibility of reducing agents to the labels bound to different regions of the protein, as well as the broad distance distributions extracted by DEER analysis, demonstrates that the global flexibility of the tertiary structure is maintained in cellular context. The use of crowding agents only partially reproduces the *E. coli* intracellular conditions. The heterogeneity of the conformational landscape of *SpUreG*, maintained in its physiological environment, suggests a role of protein flexibility for this specific GTPase enzyme, possibly related to the regulation of

promiscuous protein interactions for metal ion delivery. At the same time, the decrease of protein dynamics and *in-cell* fold compaction observed mainly in the catalytic region suggests that *SpUreG* catalytic activity requires structural rigidity to perform its physiological function. *SpUreG* folding and dynamics are the results of the compromise between two opposite conformational requirements: a prevalence of structural rigidity, needed for the GTPase function, is found in the protein catalytic core (position G9C), while backbone flexibility, required for the intrinsic regulation of activity and protein interactions, is distributed along the backbone mostly in the metal-binding (C68) and protein-protein interaction area (D158C).

Limitations of the study

In the present work, we demonstrated that the GTPase UreG presents a heterogeneous conformational landscape not only *in vitro*, as previously reported, but also in the bacterial cytoplasm. Even though the conditions tested can be considered a very good approximation of the physiological environment, some differences remain with the *in-cell* state that could, in principle, influence the protein conformational distribution and activity of UreG. Indeed, *E. coli* and *S. pasteurii* intracellular environments can be different, thus the possibility that the conformational behavior of UreG in *S. pasteurii* cytoplasm differs from the one observed in *E. coli* cannot be excluded. In addition, *S. pasteurii* expresses other urease chaperones with which UreG interacts and are not expressed in *E. coli*. The presence of cognate proteins might influence the protein conformational state, probably driving it toward the more folded state.

Acknowledgments

The authors are grateful to the EPR facilities at the French Research Infrastructure INFRANALYTICS (FR2054) and the Aix-Marseille University EPR center. We also acknowledge support from MOSBRI which has received funding from the European Union's Horizon 2020 Research and Innovation Programme under Grant Agreement N° 101004806. We acknowledge Dr. Deborah Byrne of the Protein Expression facility at the *Institut de Microbiologie de la Méditerranée* (IMM, Marseille, France) for UreG purification. We thank P. Mansuelle and R. Lebrun from Aix-Marseille University and CNRS IMM (FR 3479), Plateforme de Proteomique, 31 chemin Joseph Aiguier, F-13402 Marseille, France, for mass spectrometry measurements and analyses. We acknowledge financial support from the “Agence Nationale de la Recherche” (ANR-18-CE11-0007-01) and from the “Conseil Régional Région Sud” (A.P. PhD Fellowship EJD-2018-2021). The project leading to this publication has received funding from the A*Midex Foundation of Aix-Marseille University, funded by socio-economic partners.

Author contributions

Conceptualization, B.Z. and E.M.; Methodology, A.P., K.C.T., G.G., E.M. and H.L. Investigation, A.P., K.C.T., G.G., H.L.; Software, E.E.; Data curation, A.P., H.L., G.G.

and E. E.; Formal analysis, E.E., B.G., V.B., E. M. and B.Z.; Funding acquisition, B.G. and E.M.; Project administration, B.Z. and E.M.; Validation, Writing—original draft, A. P., V.B., B.Z. and E.M. All the authors contributed to the final version of this manuscript.

Declaration of interest

The authors declare no competing interests.

Inclusion and diversity

We support inclusive, diverse, and equitable conduct of research.

Main figure titles and legends

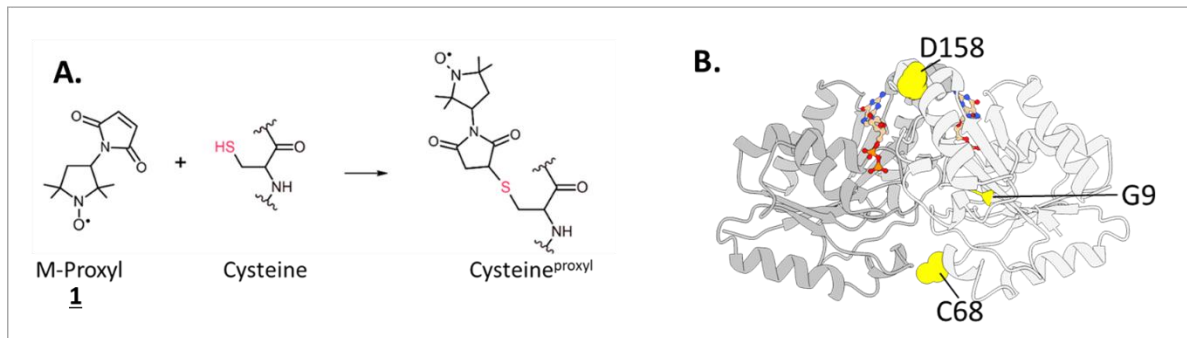


Figure 1. Site-Directed Spin Labeling of *SpUreG*. **A.** Spin-labeling reaction involving M-Proxyl (**1**) and a cysteine residue. **B.** Model structure of *SpUreG* obtained by homology modeling from *HpUreG* crystal structure³: the residues targeted for spin-labeling are indicated by yellow spheres on one monomer. See also Figure S1.

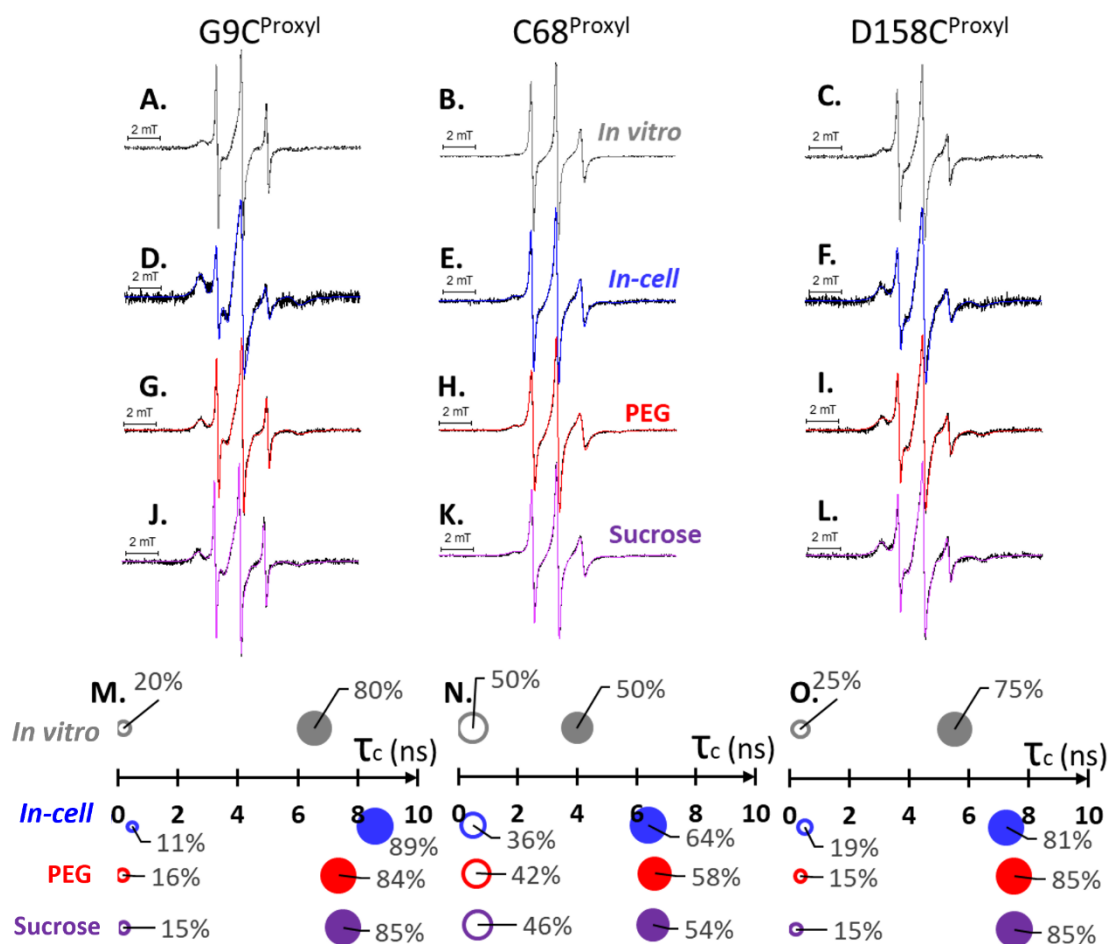


Figure 2. EPR spectra and simulation results. Room temperature, X-band CW-EPR spectra recorded for the studied *SpUreG* variants labeled with M-Proxyl (**1**) in vitro (single scan -1.5 min- in Tris Buffer 10mM, pH 7.4, panels A, B, C), and in *E. coli* cells (10 scans in 15 min for panel D, single scan in 1.5 min for panels E and F). RT, X-band CW-EPR spectra of *SpUreG* variants in presence of PEG8000 200 mg/mL

are reported in panel G, H, I; those in Sucrose 20% v/v in panels J, K, L. Experimental data are in black, while simulated ones are indicated by colored lines. Panels M, N, O summarize simulation results: τ_c extracted from the simulations are plotted on the X-axis, the percentage of each population described by a τ_c is represented as a surface of a sphere. The IDP-sharp component is reported in empty spheres, the broad-compact one as filled sphere. Simulation results of EPR spectra in the presence of crowding agents are colored as follows: blue for *in-cell* data; red for PEG8000 200 mg/mL; purple for Sucrose 20% v/v. See also Figures S2, S3, S6, S8, S12 and table S1.

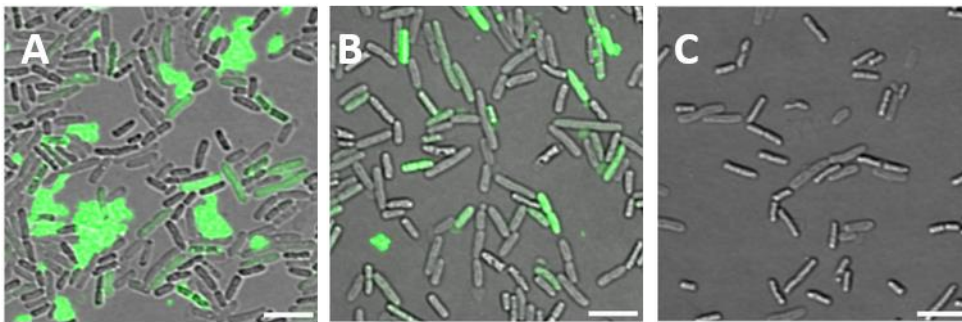


Figure 3. sfGFP internalization in *E. coli* cells followed by Fluorescence Microscopy. Transmission (DIC) and Fluorescence (MIP) image overlays of *E. coli* cells in which sfGFP was delivered by heat-shock in the presence of 50 mM (A) and 10 mM (B) Ca(II). Control experiments (C) were performed by analyzing bacteria incubated with sfGFP without performing the heat-shock. Scale bars represent 2 μ m. See also Figures S4, S5, S6 and S7.

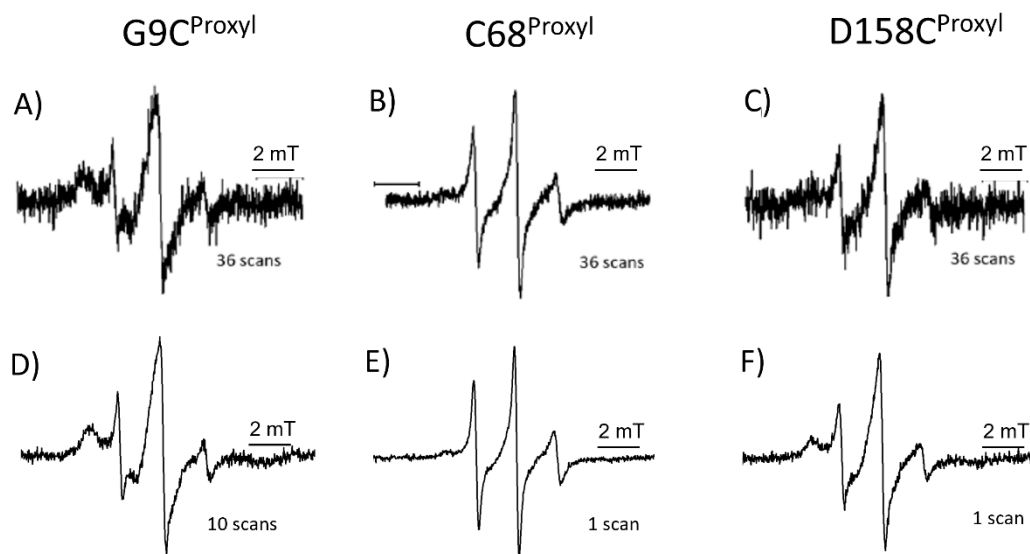


Figure 4: Comparison of EPR spectra of UreG variants delivered into *E. coli* cells by electroporation or heat-shock. Room temperature, X band, CW-EPR spectra of *SpUreG* variants delivered in *E. coli* cells by electroporation (A, B, C) or heat-shock (D, E, F), respectively. Panels A and D: *SpUreG*-G9C^{Proxyl}; Panels B and E: *SpUreG*-C68^{Proxyl}; Panels C and F: *SpUreG*-D158C^{Proxyl}. The number of scans recorded for each spectrum is indicated for each of them (36 scans for electroporation – 50 minutes of acquisition, 1-10 for heat-shock 1-15 minutes of acquisition).

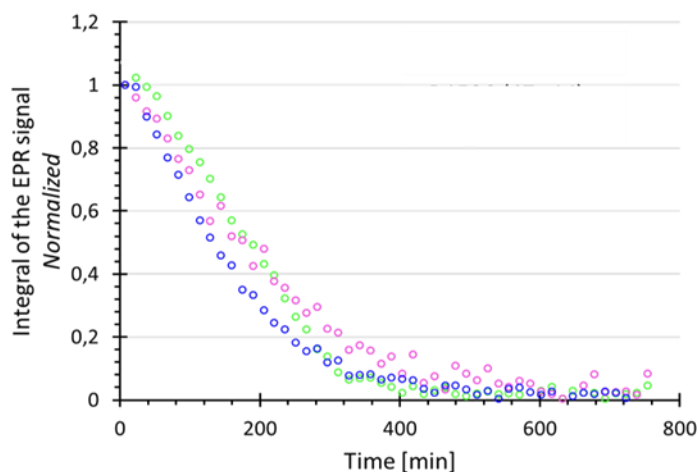


Figure 5: Nitroxide reduction profiles in the cytosol of *E. coli* cells. Normalized integrated intensity of the EPR spectra of all nitroxide-labeled *SpUreG* variants in *E. coli* over time: C68^{proxyl} in blue, G9C^{proxyl} in magenta and D158C^{proxyl} in green. Each point represents the normalized double integral of the sum of 10 consecutive EPR spectra.

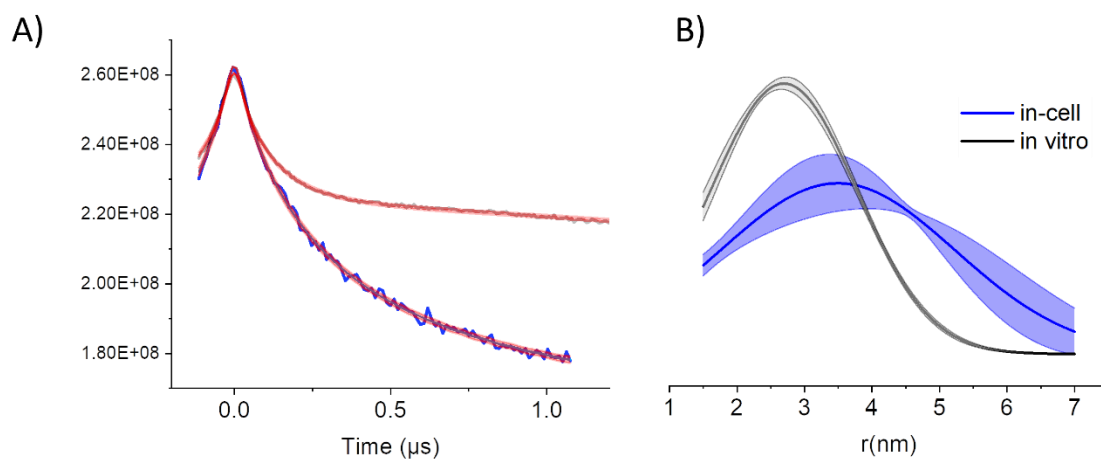


Figure 6. DEER data obtained for *SpUreG*-G9C^{proxyl}/D158C^{proxyl} in buffer (black traces) and *in-cell* (blue traces). A) Results of the DEER raw data fitting using DEERLab with a single Gaussian model.⁵⁶ The resulting distances are reported in panel B (shaded gray and blue areas represent the uncertainty). The raw time traces and the comparison of the distance distributions extracted using different models are reported in S10. See also Figures S9 and S11.

STAR Methods

1) Key resource table (in a separate word file)

2) Resource availability

Lead Contact

Further information and requests for resources and reagents should be directed to and will be fulfilled by the lead contact, Elisabetta Mileo (emileo@imm.cnrs.fr)

Materials availability

The plasmids generated in this study are available from the lead contact on reasonable request.

Data and Code Availability

- Data: All the data reported in this study are available from the lead contact on reasonable request.
- Code: Information about the two in-house developed MATLAB scripts (extract_from2D and kinetic_intensity) can be found following the links indicated in the Key Resource Table.
- Other items: Any additional information required to reanalyze the data reported in this paper is available from the [lead contact](#) upon request.

3) Methods details

SpUreG purification and spin-labeling - SpUreG-WT and its variants are cloned in a pET-3a vector and transformed in a *E. coli* BL21-DE3 strain. As previously reported, cells are cultured in LB medium until reaching OD₆₀₀=0.6 and induced by 0.5 mM IPTG for 18 hours at 20 °C.¹⁰ Cells are harvested by centrifugation at 5000 rpm 20 min at 4°C and resuspended in 60ml of 50mM Tris-HCl pH 8, containing 5mM EDTA, 2mM DTT, 10mM MgCl₂ and 20µg/ml DNase I. Cells are lysed by French pressure cell homogenizer (Stansted Fluid Power LTD) at 15000 pounds/square inch, and the supernatant is separated by centrifugation at 14000 rpm 30 minutes at 4°C. The protein purification is tag-less and involves an Anion Exchange Column previously equilibrated against 20 mM Tris-HCl pH 8 buffer containing EDTA 5 mM, 2mM DTT (AEC, Q-Sepharose 26/10, GE Healthcare). This step is followed by two Size Exclusion Chromatography columns (HiLoad Superdex XK 75 16/60 column and Superdex XK 75 13/300, GE Healthcare) against 20 mM Tris-HCl pH 8 buffer, containing NaCl 150 mM and TCEP (tris(2-carboxyethyl) phosphine) 1 mM. Prior to spin-labeling, TCEP is removed from 100 nmols of protein by PD10 desalting column (GE Healthcare) against Tris-HCl 10 mM pH7.4 buffer. The fractions containing the protein are pooled and incubated with maleimido-proxyl nitroxide (Sigma-Aldrich) in 10-fold molar excess/cysteine. A second PD10 desalting column against the same buffer described above is performed to remove the unbound spin-label's excess. The

collected fractions are then checked by EPR spectroscopy and polished by centrifugation in 2 mL Vivaspin concentrators 3kDa MWCO. The concentration of the labeled protein is evaluated by measuring the OD at 280 nm. The labeling yield (over 90%) was calculated by comparing the spin concentration (obtained by EPR spectroscopy) with the protein concentration.

sfGFP purification - sfGFP encoded in a pET22b vector tagged with a-6His tail is overexpressed in *E. coli* BL21-DE3 strain. The cells are grown in LB medium at 37°C until reaching OD₆₀₀=0.4. The overexpression is induced by addition of 0.4 mM of IPTG and growth for 4 hours at 37°C. Cells are harvested by centrifugation at 4500 rpm 20 minutes at 4°C and resuspended in Tris-HCl 20mM pH 7.4 buffer, containing NaCl 150mM and protease inhibitors EDTA-free cocktail (Roche). After three passages into EmulsiFlex (Avestin) at 1500 psi, the supernatant is separated by centrifugation at 45000 rpm for 50 minutes.

The supernatant is loaded in a Ni-NTA superflow column 5 mL (Qiagen) equilibrated with Tris-HCl 20 mM pH 7.4, NaCl 150 mM, Imidazole 10 mM. sfGFP elutes in Tris-HCl 20 mM pH 7.4, NaCl 150 mM, Imidazole 200 mM. Fractions containing the protein are then dialyzed in a 3 kDa MWCO membrane against 500 mL Tris-HCl 20 mM pH 7.4, NaCl 150 mM for 2 hours, renovating the buffer every 30 minutes. Protein concentration was estimated using absorbance at 485 nm and an extinction coefficient $\epsilon_{400}=83300 \text{ M}^{-1}\text{cm}^{-1}$ (<http://us.expasy.org/cgi-bin/protparam>).

Preparation of competent *E. coli* cells for heat-shock - An overnight pre-culture of *E. coli* NEB® 5-alpha cells is diluted to a final OD₆₀₀= 0.05 into 20 mL of LB medium and cultured at 37 °C until reaching OD₆₀₀= 0.6. The growth is, then, stopped by chilling the cells at 4 °C on ice for at least 30 minutes. Bacterial cells are harvested by centrifugation at 4000 $\times g$ at 4 °C for 15 minutes and re-suspended in 10 mL of sterile CaCl₂ 50 mM. This mixture is incubated for 2 hours at 4 °C. Finally, bacterial cells are harvested 3800 $\times g$ 10 minutes at 4 °C and resuspended in CaCl₂ 10 mM to obtain a final concentration between 4–7 * 10¹⁰ cells/mL. Cells are incubated at 4 °C for at least 20 minutes and used for an in-cell EPR experiment in the same day.

Preparation of competent *E. coli* cells for electroporation - Electrocompetent cells were prepared as previously reported.³³ An overnight pre-culture of *E. coli* NEB® 5-alpha cells is inoculated in 100 mL LB medium to a final OD₆₀₀= 0.05 and incubated at 37 °C until reaching OD₆₀₀= 0.9. After chilling the cells at 4 °C on ice for at least 30 minutes, they are harvested by centrifugation at 4000 $\times g$ for 10 minutes at 4 °C and re-suspended in 100mL of sterile MilliQ water + 10% glycerol. This step is repeated two times, reducing the volume of the washes to 60 mL and 50 mL, respectively. Finally, bacterial cells are resuspended in sterile MilliQ water + 10% glycerol. The cell number was estimated between 4–7 * 10¹⁰ cells/mL. Cells can be aliquoted and stored at –80 °C.

Protein delivery by heat-shock and electroporation - As first step, 20 μL of competent cells are incubated with 20 μL of labeled protein 10 minutes on ice. For electroporation, the protein

must be without salt to avoid arching. For electroporation, the protein-cells mixture is, then, transferred into a pre-chilled 1 mm-gap cuvette (VRW) and electroporated in a Gene Pulser Xcell™ from Bio-Rad, using the following parameters: 1800 V/cm, 200 Ω , 25 μ F, 1 msec pulse. For heat shock, the mixture is incubated 2 minutes at 42 °C and 2 minutes at 4 °C. In both protocols, the cells membrane integrity is recovered by addition of 500 μ L of pre-warmed SOC.

Cells are then washed by centrifugation at 3200 $\times g$, 2 minutes at 4 °C three times: 500 μ L of PBS (Phosphate Buffer 10 mM pH 7.5, KCl 2.7 mM, NaCl 137 mM) + 0.005% Triton solution, in the first wash, 500 μ L of PBS until the excess of not internalized protein is completely removed (4 washes for heatshock and 3 washes for electroporation). For CW-EPR at room temperature the pellet is resuspended in 50 μ L of PBS with 1% LT-Agarose (Euromedex) and transferred in an EPR quartz capillary. For confocal microscopy 4 μ L of sample are transferred on an agar pad.

Fluorescence Microscopy - Imaging was performed using an inverted fluorescence confocal microscope, Olympus FV1000-IX81 with an 100X/1.40 objective oil immersion. Images were acquired using a laser excitation at 488nm and emission fluorescence was recovered in the range 500-600nm. The transmission image is also recovered in order to determine the outline of the bacteria.

Fluorescence Microscopy Image analysis - The transmission images were first segmented using the Napari (0.4.16) viewer and the MiSiC plugin <https://pypi.org/project/misic-napari/>, in order to detect each bacterium individually. Then the fluorescence was measured using Fiji (1.53s) for each bacterium and divided by the average fluorescence of the image background, to obtain a signal to noise ratio. The ratios were sorted in ascending order and plotted in a graph for the conditions tested (heat shock of sfGFP and *E. coli* cells in CaCl₂ 50mM or CaCl₂ 10mM and *E. coli* cells in CaCl₂ 10mM in contact with sfGFP).

CW-EPR experiments in vitro and in crowded solutions - All the room temperature CW-EPR experiments are recorded at room temperature on a spectrometer Elexsys 500 (Bruker) equipped with a Super High Q sensitivity resonator at X band (9.9GHz). Samples are injected in a quartz capillary whose sensible volume was 40 μ L and recorded using the following parameters: microwaves power = 10mW; magnetic field modulation amplitude=1G; field sweep=150G; receiver gain=60dB. Simulations of CW-EPR spectra, performed using SimLabel,³⁸ a GUI of EasySpin,^{8,9} are detailed in the Supplemental Information, from Figure S11 to S29.

In crowding experiments, crowding agents are dissolved in 10 mL of 10 mM Tris buffer pH 7.4 to obtain the desired concentration. To do not dilute the solution, 5 μ L of protein are added to this solution to obtain a final concentration of 50 μ M in 50 μ L.

The reduction profiles presented in Figure 5 result from 2D experiments (field sweep and time): for field sweep EPR spectra acquisition we used the same parameters described before in this section, while the delay between the acquisition of each spectrum was of 90 s.

DEER experiments - For in vitro studies, SpUreG_C68A-G9C^{proxyl}/D158C^{proxyl} was diluted in a buffer containing 30% of glycerol, as a cryoprotector. Concerning in-cell EPR samples, after the delivery of the protein inside the cell by heat-shock or electroporation, the excess of not internalized protein is removed by washing the pellet with deuterated PBS four times as described for CW-EPR samples. Cells are then resuspended in deuterated PBS enriched with 30% of glycerol D8, transferred in a quartz Q-band capillary and flash-frozen in liquid nitrogen. The time between the delivery trigger and the freezing was between 12-15 minutes. DEER distance measurements were performed at 60K on a Bruker ELEXSYS E580 spectrometer equipped with an Oxford helium temperature regulation unit at Q-band using the standard EN 5107D2 resonator. All the measurements were performed at 60K on 20 μ L of sample. The DEER traces were, then, analyzed using DeerLab software.⁵⁶ as recommended in literature⁵⁷ (<https://github.com/JeschkeLab/DeerLab>, ETH, Zürich, Switzerland).

Quantification and Statistical analysis

Data showed in Figure 5 were analysed using in-house developed MATLAB scripts, “extract_from2D” and “kinetic_intensity”.

Extract_from2D was used to sum ten consecutive spectra of the 2D EPR experiments (normally characterized by between 500 and 700 spectra) in order to obtain a 2D experiment having ten times less spectra but a higher signal to noise ratio. This home-made MATLAB software uses some EasySpin functions³⁹ (extract_from2D, mode 2D/group spectra, available here: <https://bip.cnrs.fr/epr-facility/software-and-scripts/>). Spectra treated with extract_from2D were then analysed using kinetic_intensity, a MATLAB home made software using some EasySpin functions³⁹ (available here: <https://bip.cnrs.fr/epr-facility/software-and-scripts/>). This script enables: *i*) to plot the absorption spectrum (numerically obtained) of each experimental spectra of a 2D experiment, *ii*) to apply a baseline correction, managed by the user, on the absorption spectra, *iii*) to automatically extract the numerical integrated intensity of the corrected spectra and *iv*) to plot the obtained intensities versus the time of the spectra acquisition (automatically extracted).

References.

1. Maroney, M.J., and Ciurli, S. (2014). Nonredox nickel enzymes. *Chem Rev* *114*, 4206-4228. 10.1021/cr4004488.
2. Zambelli, B., Musiani, F., Benini, S., and Ciurli, S. (2011). Chemistry of Ni²⁺ in urease: sensing, trafficking, and catalysis. *Acc Chem Res* *44*, 520-530. 10.1021/ar200041k.
3. Merloni, A., Dobrovolska, O., Zambelli, B., Agostini, F., Bazzani, M., Musiani, F., and Ciurli, S. (2014). Molecular landscape of the interaction between the urease accessory proteins UreE and UreG. *Biochim Biophys Acta* *1844*, 1662-1674. 10.1016/j.bbapap.2014.06.016.
4. Yuen, M.H., Fong, Y.H., Nim, Y.S., Lau, P.H., and Wong, K.-B. (2017). Structural insights into how GTP-dependent conformational changes in a metallochaperone UreG facilitate urease maturation. *Proceedings of the National Academy of Sciences* *114*, E10890-E10898. 10.1073/pnas.1712658114.
5. Zambelli, B., Turano, P., Musiani, F., Neyroz, P., and Ciurli, S. (2009). Zn²⁺-linked dimerization of UreG from *Helicobacter pylori*, a chaperone involved in nickel trafficking and urease activation. *Proteins* *74*, 222-239. 10.1002/prot.22205.
6. Zambelli, B., Cremades, N., Neyroz, P., Turano, P., Uversky, V.N., and Ciurli, S. (2012). Insights in the (un)structural organization of *Bacillus pasteurii* UreG, an intrinsically disordered GTPase enzyme. *Molecular bioSystems* *8*, 220-228. 10.1039/c1mb05227f.
7. Real-Guerra, R., Staniscuaski, F., Zambelli, B., Musiani, F., Ciurli, S., and Carlini, C.R. (2012). Biochemical and structural studies on native and recombinant Glycine max UreG: a detailed characterization of a plant urease accessory protein. *Plant molecular biology* *78*, 461-475. 10.1007/s11103-012-9878-1.
8. D'Urzo, A., Santambrogio, C., Grandori, R., Ciurli, S., and Zambelli, B. (2014). The conformational response to Zn(II) and Ni(II) binding of *Sporosarcina pasteurii* UreG, an intrinsically disordered GTPase. *J Biol Inorg Chem* *19*, 1341-1354. 10.1007/s00775-014-1191-9.
9. Miraula, M., Ciurli, S., and Zambelli, B. (2015). Intrinsic disorder and metal binding in UreG proteins from Archae hyperthermophiles: GTPase enzymes involved in the activation of Ni(II) dependent urease. *J Biol Inorg Chem* *20*, 739-755. 10.1007/s00775-015-1261-7.
10. Zambelli, B., Stola, M., Musiani, F., De Vriendt, K., Samyn, B., Devreese, B., Van Beeumen, J., Turano, P., Dikiy, A., Bryant, D.A., and Ciurli, S. (2005). UreG, a chaperone in the urease assembly process, is an intrinsically unstructured GTPase that specifically binds Zn²⁺. *J Biol Chem* *280*, 4684-4695. 10.1074/jbc.M408483200.
11. Zambelli, B., Mazzei, L., and Ciurli, S. (2020). Intrinsic disorder in the nickel-dependent urease network. *Progress in molecular biology and translational science* *174*, 307-330. 10.1016/bs.pmbts.2020.05.004.
12. Palombo, M., Bonucci, A., Etienne, E., Ciurli, S., Uversky, V.N., Guigliarelli, B., Belle, V., Mileo, E., and Zambelli, B. (2017). The relationship between folding and activity in UreG, an intrinsically disordered enzyme. *Scientific reports* *7*, 5977. 10.1038/s41598-017-06330-9.
13. Pierro, A., Etienne, E., Gerbaud, G., Guigliarelli, B., Ciurli, S., Belle, V., Zambelli, B., and Mileo, E. (2020). Nickel and GTP Modulate *Helicobacter pylori* UreG Structural Flexibility. *Biomolecules* *10*, 1062.
14. Torricella, F., Pierro, A., Mileo, E., Belle, V., and Bonucci, A. (2021). Nitroxide spin labels and EPR spectroscopy: A powerful association for protein dynamics studies. *Biochimica*

- et biophysica acta. Proteins and proteomics 1869, 140653. 10.1016/j.bbapap.2021.140653.
15. Jassoy, J.J., Berndhäuser, A., Duthie, F., Kühn, S.P., Hagelueken, G., and Schiemann, O. (2017). Versatile Trityl Spin Labels for Nanometer Distance Measurements on Biomolecules In Vitro and within Cells. *Angew. Chem. Int. Ed.* 56, 177-181. doi:10.1002/anie.201609085.
 16. Singewald, K., Hunter, H., Cunningham, T.F., Ruthstein, S., and Saxena, S. (2023). Measurement of Protein Dynamics from Site Directed Cu(II) Labeling. *Analysis & Sensing* 3, e202200053. <https://doi.org/10.1002/anse.202200053>.
 17. Banerjee, D., Yagi, H., Huber, T., Otting, G., and Goldfarb, D. (2012). Nanometer-Range Distance Measurement in a Protein Using Mn²⁺ Tags. *The Journal of Physical Chemistry Letters* 3, 157-160. 10.1021/jz201521d.
 18. Prokopiou, G., Lee, M.D., Collauto, A., Abdelkader, E.H., Bahrenberg, T., Feintuch, A., Ramirez-Cohen, M., Clayton, J., Swarbrick, J.D., Graham, B., et al. (2018). Small Gd(III) Tags for Gd(III)–Gd(III) Distance Measurements in Proteins by EPR Spectroscopy. *Inorg. Chem.* 57, 5048-5059. 10.1021/acs.inorgchem.8b00133.
 19. Lorenzi, M., Puppo, C., Lebrun, R., Lignon, S., Roubaud, V., Martinho, M., Mileo, E., Tordo, P., Marque, S.R., Gontero, B., et al. (2011). Tyrosine-targeted spin labeling and EPR spectroscopy: an alternative strategy for studying structural transitions in proteins. *Angew Chem Int Ed Engl* 50, 9108-9111. 10.1002/anie.201102539.
 20. Mileo, E., Etienne, E., Martinho, M., Lebrun, R., Roubaud, V., Tordo, P., Gontero, B., Guigliarelli, B., Marque, S.R., and Belle, V. (2013). Enlarging the panoply of site-directed spin labeling electron paramagnetic resonance (SDSL-EPR): sensitive and selective spin-labeling of tyrosine using an isoindoline-based nitroxide. *Bioconjugate chemistry* 24, 1110-1117. 10.1021/bc4000542.
 21. Gmeiner, C., Klose, D., Mileo, E., Belle, V., Marque, S.R.A., Dorn, G., Allain, F.H.T., Guigliarelli, B., Jeschke, G., and Yulikov, M. (2017). Orthogonal Tyrosine and Cysteine Site-Directed Spin Labeling for Dipolar Pulse EPR Spectroscopy on Proteins. *J Phys Chem Lett*, 4852-4857. 10.1021/acs.jpcclett.7b02220.
 22. Jeschke, G. (2018). The contribution of modern EPR to structural biology. *Emerging Topics in Life Sciences*. 10.1042/etls20170143.
 23. Goldfarb, D. (2022). Exploring protein conformations in vitro and in cell with EPR distance measurements. *Curr. Opin. Struc. Biol.* 75, 102398. <https://doi.org/10.1016/j.sbi.2022.102398>.
 24. Bonucci, A., Ouari, O., Guigliarelli, B., Belle, V., and Mileo, E. (2020). In-Cell EPR: Progress towards Structural Studies Inside Cells. *ChemBioChem* 21, 451-460. 10.1002/cbic.201900291.
 25. Theillet, F.-X. (2022). In-Cell Structural Biology by NMR: The Benefits of the Atomic Scale. *Chemical Reviews* 122, 9497-9570. 10.1021/acs.chemrev.1c00937.
 26. Pierro, A., Bonucci, A., Normanno, D., Ansaldi, M., Pilet, E., Ouari, O., Guigliarelli, B., Etienne, E., Gerbaud, G., Magalon, A., et al. (2022). Probing the Structural Dynamics of a Bacterial Chaperone in Its Native Environment by Nitroxide-Based EPR Spectroscopy. *Chemistry – A European Journal* 28, e202202249. <https://doi.org/10.1002/chem.202202249>.
 27. Karthikeyan, G., Bonucci, A., Casano, G., Gerbaud, G., Abel, S., Thomé, V., Kodjabachian, L., Magalon, A., Guigliarelli, B., Belle, V., et al. (2018). A Bioresistant Nitroxide Spin Label for In-Cell EPR Spectroscopy: In Vitro and In Oocytes Protein

- Structural Dynamics Studies. *Angew. Chem. Int. Ed.* *57*, 1366-1370. doi:10.1002/anie.201710184.
28. Martorana, A., Bellapadrona, G., Feintuch, A., Di Gregorio, E., Aime, S., and Goldfarb, D. (2014). Probing protein conformation in cells by EPR distance measurements using Gd³⁺ spin labeling. *J Am Chem Soc* *136*, 13458-13465. 10.1021/ja5079392.
 29. Schmidt, M.J., Borbas, J., Drescher, M., and Summerer, D. (2014). A genetically encoded spin label for electron paramagnetic resonance distance measurements. *J Am Chem Soc* *136*, 1238-1241. 10.1021/ja411535q.
 30. Schmidt, M.J., Fedoseev, A., Bücker, D., Borbas, J., Peter, C., Drescher, M., and Summerer, D. (2015). EPR Distance Measurements in Native Proteins with Genetically Encoded Spin Labels. *ACS Chemical Biology* *10*, 2764-2771. 10.1021/acscchembio.5b00512.
 31. Torricella, F., Bonucci, A., Polykretis, P., Cencetti, F., and Banci, L. (2021). Rapid protein delivery to living cells for biomolecular investigation. *Biochem. Biophys. Res. Commun.* *570*, 82-88. <https://doi.org/10.1016/j.bbrc.2021.07.006>.
 32. Torricella, F., Barbieri, L., Bazzurro, V., Diaspro, A., and Banci, L. (2022). Protein delivery to living cells by thermal stimulation for biophysical investigation. *Scientific reports* *12*, 17190. 10.1038/s41598-022-21103-9.
 33. Pierro, A., Bonucci, A., Normanno, D., Ansaldi, M., Pilet, E., Ouari, O., Guigliarelli, B., Etienne, E., Gerbaud, G., Magalon, A., et al. Probing Structural Dynamics of a Bacterial Chaperone in Its Native Environment by Nitroxide-Based EPR Spectroscopy. *Chemistry – A European Journal* *n/a*. <https://doi.org/10.1002/chem.202202249>.
 34. Pierro, A., Bonucci, A., Normanno, D., Ansaldi, M., Pilet, E., Ouari, O., Guigliarelli, B., Etienne, E., Gerbaud, G., Magalon, A., et al. (2022). Probing the Structural Dynamics of a Bacterial Chaperone in Its Native Environment by Nitroxide-Based EPR Spectroscopy. *Chemistry – A European Journal* *n/a*, e202202249. <https://doi.org/10.1002/chem.202202249>.
 35. Yang, Y., Yang, F., Gong, Y.-J., Bahrenberg, T., Feintuch, A., Su, X.-C., and Goldfarb, D. (2018). High Sensitivity In-Cell EPR Distance Measurements on Proteins using an Optimized Gd(III) Spin Label. *The Journal of Physical Chemistry Letters* *9*, 6119-6123. 10.1021/acs.jpcllett.8b02663.
 36. Pierro, A., and Drescher, M. (2023). Dance with spins: site-directed spin labeling coupled to electron paramagnetic resonance spectroscopy directly inside cells. *Chem. Commun.* 10.1039/D2CC05907J.
 37. Bellucci, M., Zambelli, B., Musiani, F., Turano, P., and Ciurli, S. (2009). Helicobacter pylori UreE, a urease accessory protein: specific Ni(2+)- and Zn(2+)-binding properties and interaction with its cognate UreG. *The Biochemical journal* *422*, 91-100. 10.1042/bj20090434.
 38. Etienne, E., Le Breton, N., Martinho, M., Mileo, E., and Belle, V. (2017). SimLabel: a graphical user interface to simulate continuous wave EPR spectra from site-directed spin labeling experiments. *Magnetic resonance in chemistry : MRC* *55*, 714-719. 10.1002/mrc.4578.
 39. Stoll, S., and Schweiger, A. (2006). EasySpin, a comprehensive software package for spectral simulation and analysis in EPR. *Journal of magnetic resonance (San Diego, Calif. : 1997)* *178*, 42-55. 10.1016/j.jmr.2005.08.013.
 40. Mileo, E., Lorenzi, M., Eroles, J., Lignon, S., Puppo, C., Le Breton, N., Etienne, E., Marque, S.R., Guigliarelli, B., Gontero, B., and Belle, V. (2013). Dynamics of the intrinsically disordered protein CP12 in its association with GAPDH in the green alga

- Chlamydomonas reinhardtii: a fuzzy complex. *Molecular bioSystems* 9, 2869-2876. 10.1039/c3mb70190e.
41. Zambelli, B., Musiani, F., Savini, M., Tucker, P., and Ciurli, S. (2007). Biochemical studies on Mycobacterium tuberculosis UreG and comparative modeling reveal structural and functional conservation among the bacterial UreG family. *Biochemistry* 46, 3171-3182. 10.1021/bi6024676.
 42. López, C.J., Fleissner, M.R., Guo, Z., Kusnetzow, A.K., and Hubbell, W.L. (2009). Osmolyte perturbation reveals conformational equilibria in spin-labeled proteins. *Protein science : a publication of the Protein Society* 18, 1637-1652. 10.1002/pro.180.
 43. Hubbell, W.L., Lopez, C.J., Altenbach, C., and Yang, Z. (2013). Technological advances in site-directed spin labeling of proteins. *Curr Opin Struct Biol* 23, 725-733. 10.1016/j.sbi.2013.06.008.
 44. Flores Jiménez, R.H., Do Cao, M.A., Kim, M., and Cafiso, D.S. (2010). Osmolytes modulate conformational exchange in solvent-exposed regions of membrane proteins. *Protein science : a publication of the Protein Society* 19, 269-278. 10.1002/pro.305.
 45. Jagtap, A.P., Krstic, I., Kunjir, N.C., Hansel, R., Prisner, T.F., and Sigurdsson, S.T. (2015). Sterically shielded spin labels for in-cell EPR spectroscopy: analysis of stability in reducing environment. *Free radical research* 49, 78-85. 10.3109/10715762.2014.979409.
 46. Speer, S.L., Stewart, C.J., Sapir, L., Harries, D., and Pielak, G.J. (2022). Macromolecular Crowding Is More than Hard-Core Repulsions. *Annual Review of Biophysics* 51, 267-300. 10.1146/annurev-biophys-091321-071829.
 47. Sharp, K.A. (2016). Unpacking the origins of in-cell crowding. *Proceedings of the National Academy of Sciences* 113, 1684-1685. doi:10.1073/pnas.1600098113.
 48. Akabayov, B., Akabayov, S.R., Lee, S.-J., Wagner, G., and Richardson, C.C. (2013). Impact of macromolecular crowding on DNA replication. *Nature Communications* 4, 1615. 10.1038/ncomms2620.
 49. Stagg, L., Zhang, S.-Q., Cheung, M.S., and Wittung-Stafshede, P. (2007). Molecular crowding enhances native structure and stability of α/β protein flavodoxin. *Proceedings of the National Academy of Sciences* 104, 18976-18981. doi:10.1073/pnas.0705127104.
 50. Zhou, B.R., Zhou, Z., Hu, Q.L., Chen, J., and Liang, Y. (2008). Mixed macromolecular crowding inhibits amyloid formation of hen egg white lysozyme. *Biochim Biophys Acta* 1784, 472-480. 10.1016/j.bbapap.2008.01.004.
 51. Street, T.O., Bolen, D.W., and Rose, G.D. (2006). A molecular mechanism for osmolyte-induced protein stability. *Proceedings of the National Academy of Sciences* 103, 13997-14002. doi:10.1073/pnas.0606236103.
 52. Parray, Z.A., Hassan, M.I., Ahmad, F., and Islam, A. (2020). Amphiphilic nature of polyethylene glycols and their role in medical research. *Polym. Test.* 82, 106316. <https://doi.org/10.1016/j.polymertesting.2019.106316>.
 53. Jeschke, G. (2018). MMM: A toolbox for integrative structure modeling. *Protein Sci.* 27, 76-85. <https://doi.org/10.1002/pro.3269>.
 54. Kucher, S., Elsner, C., Safonova, M., Maffini, S., and Bordignon, E. (2021). In-Cell Double Electron–Electron Resonance at Nanomolar Protein Concentrations. *The Journal of Physical Chemistry Letters* 12, 3679-3684. 10.1021/acs.jpcllett.1c00048.
 55. Joseph, B., Sikora, A., and Cafiso, D.S. (2016). Ligand Induced Conformational Changes of a Membrane Transporter in E. coli Cells Observed with DEER/PELDOR. *Journal of the American Chemical Society* 138, 1844-1847. 10.1021/jacs.5b13382.

56. Fábregas Ibáñez, L., Jeschke, G., and Stoll, S. (2020). DeerLab: a comprehensive software package for analyzing dipolar electron paramagnetic resonance spectroscopy data. *Magn. Reson.* *1*, 209-224. 10.5194/mr-1-209-2020.
57. Schiemann, O., Heubach, C.A., Abdullin, D., Ackermann, K., Azarkh, M., Bagryanskaya, E.G., Drescher, M., Endeward, B., Freed, J.H., Galazzo, L., et al. (2021). Benchmark Test and Guidelines for DEER/PELDOR Experiments on Nitroxide-Labeled Biomolecules. *Journal of the American Chemical Society* *143*, 17875-17890. 10.1021/jacs.1c07371.